



Dust emission from the first massive galaxies

M.E. De Rossi^{1,2}, G.H. Rieke³, I. Shivaee³, V. Bromm⁴ & J. Lyu³

¹ *Universidad de Buenos Aires, Facultad de Ciencias Exactas y Naturales y Ciclo Básico Común. Buenos Aires, Argentina*

² *CONICET-Universidad de Buenos Aires, Instituto de Astronomía y Física del Espacio (IAFE). Buenos Aires, Argentina*

³ *Steward Observatory, Department of Astronomy, University of Arizona, 933 North Cherry Avenue, Tucson, AZ 85721*

⁴ *Department of Astronomy, University of Texas at Austin, 2511 Speedway, Austin, TX 78712, USA*

Contact / mariaemilia.dr@gmail.com, ghrieke@gmail.com

Resumen / Comparamos las distribuciones espectrales de energía (SEDs, por sus siglas en inglés) de galaxias observadas en el infrarojo lejano (FIR, por sus siglas en inglés) a $z \sim 6$ y las predicciones teóricas para las primeras galaxias masivas de población II (Pop II, por sus siglas en inglés). Las SEDs en el FIR a $z \gtrsim 5$ son anchas y están desplazadas hacia longitudes de onda más azules comparadas con galaxias a $z \sim 3$. Mediante la implementación de un modelo analítico para la emisión por polvo de galaxias Pop II, pudimos reproducir el comportamiento observado como consecuencia de las altas densidades de energía y la composición de polvo rica en silicio de las galaxias modeladas a alto z . Como se notó en un trabajo previo, la falta de naturaleza de cuerpo negro de las SEDs de galaxias a $z \sim 6$ debería tenerse en cuenta cuando se interpretan las mediciones de las luminosidades en el FIR para evitar subestimar las tasas de formación estelar.

Abstract / We compare observed far-infrared (FIR) galaxy spectral energy distributions (SEDs) at $z \sim 6$ and theoretical predictions for first massive population II (Pop II) galaxies. Observed FIR SEDs at $z \gtrsim 5$ are broad and shifted to bluer wavelengths when compared to galaxies at $z \sim 3$. By implementing an analytical model for dust emission from Pop II massive galaxies, we were able to reproduce the observed behaviour as a consequence of the high energy densities and silicate-rich dust composition of high- z model galaxies. As noted in a previous work, the non-blackbody nature of galaxy SEDs at $z \sim 6$ should be taken into account when interpreting measurements of FIR luminosities to avoid underestimating star formation rates.

Keywords / galaxies: high-redshift — galaxies: evolution — galaxies: formation — galaxies: star formation — cosmology: theory

1. Introduction

The behaviour of the far-infrared (FIR) spectral energy distributions (SEDs) of star-forming (SF) galaxies at high redshifts ($z \gtrsim 3$) is under debate in the literature. Given the relatively little information available, these SEDs have been characterized in simplified ways. By using indirect arguments, Faisst et al. (2017) concluded that galaxies at very high z show generally "hotter" SEDs than galaxies in the Local Universe ($0 \leq z \lesssim 0.1$). According to Lyu et al. (2016), after subtracting the AGN contribution, the host FIR SEDs of $z \sim 5$ –6 quasars are better described by the relatively warm SED of the metal-poor starbursting galaxy Haro 11 ($z \approx 0.02$), instead of the normal metal-rich SF templates used at $z \lesssim 2$ –3 or modified blackbodies.

De Rossi et al. (2018) modelled the FIR SEDs corresponding to massive Population (Pop) II galaxies (formed after the Pop III stage) during the first phase of significant star formation, finding that these SEDs are significantly shifted to bluer ("warmer") wavelengths compared to the SEDs of local galaxies. In addition, adopting a silicate-rich interstellar dust composition with a small percentage of carbon dust, the theoretical SEDs have very similar behavior to that of Haro

11. Given its moderately-low metallicity and very young stellar population, Haro 11 probably describes the relevant properties in young massive Pop II galaxies at high z . In particular, De Rossi et al. (2018) reported a progression with z in the SEDs of observed galaxies, from those resembling local ones at $2 \lesssim z < 4$ to a more similar behaviour to Haro 11 at $5 \lesssim z \lesssim 7$. Such variations should be taken into account when estimating total infrared luminosities at $z \gtrsim 5$ from measurements close to $\lambda \sim 1$ mm.

In this article, we extend the work by De Rossi et al. (2018) performing a detailed comparison between the theoretical SED, the observed data and different templates SEDs at the extreme redshift end ($z = 5$ –7).

2. Dust model

We adapt the model of De Rossi & Bromm (2017) to conditions in very luminous galaxies being detected in the FIR at $z \sim 6$ (see De Rossi et al. 2018, for more details). A model galaxy consists of a dark matter halo hosting a central cluster of Pop II stars, surrounded by a mixed phase of gas and dust. We assume a dust-to-metal mass ratio $D/M = 0.02$, a gas metallicity of

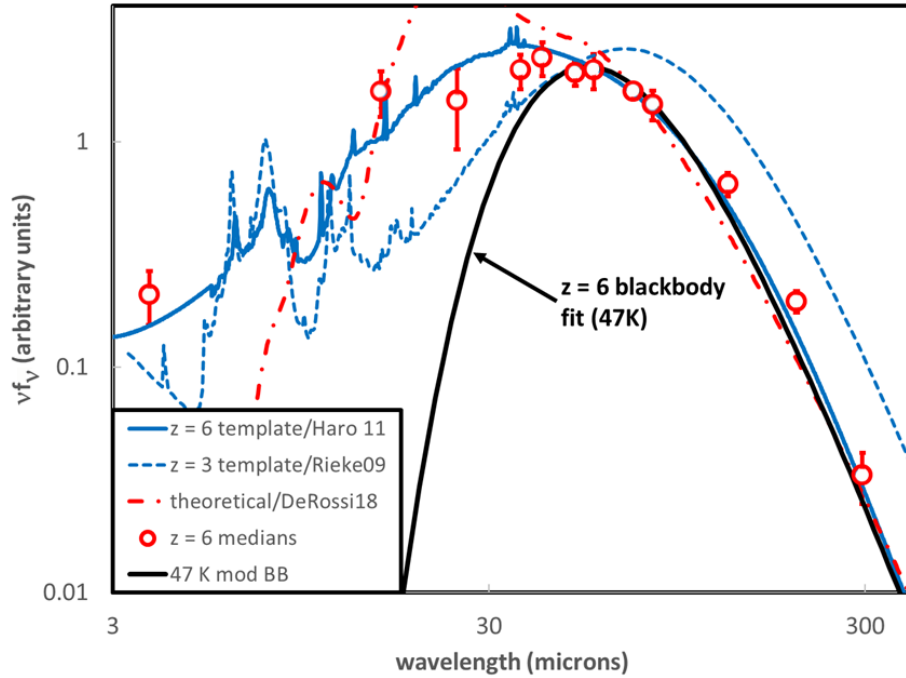


Figure 1: Comparison between theoretical and observed FIR SEDs at high z . Different curves and symbols depict medians of the measurements at $z \sim 6$ shifted to the rest-frame (open red circles, 1σ error bars), the Haro 11 template (solid blue line), the template that fits best at $z = 2 - 4$ (dashed blue line), a standard modified blackbody fit for $z = 6$ ($T = 47$ K, $\beta = 1.6$, solid black line), and the theoretical model preferred by De Rossi et al. (2018) (UM-D-20 model for silicate dust with 10% carbon, dot-dashed red line).

$Z_g = 0.33 Z_\odot$ and a star formation efficiency of $\eta = 0.01$.

We considered the different silicon-based dust models (Cherchneff & Dwek, 2010) implemented by De Rossi & Bromm (2017), but with 10% of the total luminosity contributed by carbon. We adopted the ‘standard’ grain-size distribution used in Ji et al. (2014). A dust temperature (T_d) was determined assuming thermal equilibrium and the dust emissivity was estimated by applying the Kirchhoff’s law for the estimated T_d profile.

3. Results

Fig. 1 compares the theoretical model preferred by De Rossi et al. (2018) (UM-D-20 with 10% carbon, dot-dashed red line) with the medians of the measurements at $z \sim 6$ shifted to the rest-frame (open red circles, see De Rossi et al. 2018 for details about individual and stacked observational data). Other curves in Fig. 1 depict the Haro 11 template (solid blue line), the template that fits best luminous galaxies at $z = 2 - 4$ (Rieke et al., 2009) (dashed blue line), and a standard modified blackbody fit for $z = 6$ ($T = 47$ K, $\beta = 1.6$), which is commonly used to interpret the ALMA 1 mm measurements. The modified blackbody has been fitted to SEDs within the wavelength range accessible to ALMA at $z = 6$. To show relative luminosity in logarithmic wavelength bins, the SEDs are represented by νf_ν units with an arbitrary normalization.

We see that observed galaxies at $z \sim 6$ have broad SEDs, which are bluer than those typical at lower z .

It is clear that observed trends are well reproduced by the continuum predicted by the theoretical model of De Rossi et al. (2018). Departures from the model occur around $20 \mu\text{m}$ due to silicate emission and at wavelengths $\leq 8 \mu\text{m}$ where hot dust, probably in close proximity to the hot stars, contributes to the observed fluxes. The model behavior is due to higher dust temperatures reached at higher z , caused mainly by the high energy densities inside luminous galaxies. In addition, their dominant silicate dust has high radiative efficiency at $\lambda = 8 - 60 \mu\text{m}$, augmenting the effects of the high energy density. The high energy densities inside the first massive galaxies results from the extremely high luminosities of their young stellar component ($\sim 10^{13} L_\odot$) combined with their compact sizes (Spilker et al., 2016).

Fig. 1 also shows that the SED template based on the local galaxy Haro 11 constitutes a good representation of the $z \sim 6$ data and is also well described by the theoretical model. As discussed in De Rossi et al. (2018), this is expected as the interstellar medium conditions in Haro 11 are in reasonable agreement with those corresponding to luminous infrared galaxies at $z \sim 6$. Thus, De Rossi et al. (2018) proposed the Haro 11 SED as a proxy template to describe the trends of FIR SEDs at high z . On the other hand, a modified blackbody fit (solid black line) provides a good representation of the data within the range of rest wavelengths accessible with ALMA at submm- and mm-wave observations ($\lambda > 40 \mu\text{m}$), but leads to an underestimation of total infrared luminosities – and star formation rates – by a factor of 2. Other commonly used templates also

result in substantial underestimates of the infrared luminosities based just on ALMA measurements near 1 mm compared with the estimate using the Haro 11 template, as shown in Figure 2. Here we plot the ratio of deduced FIR luminosity to the Band 7 flux density (in mJy) as a function of redshift, as it is predicted by a number of commonly used templates.

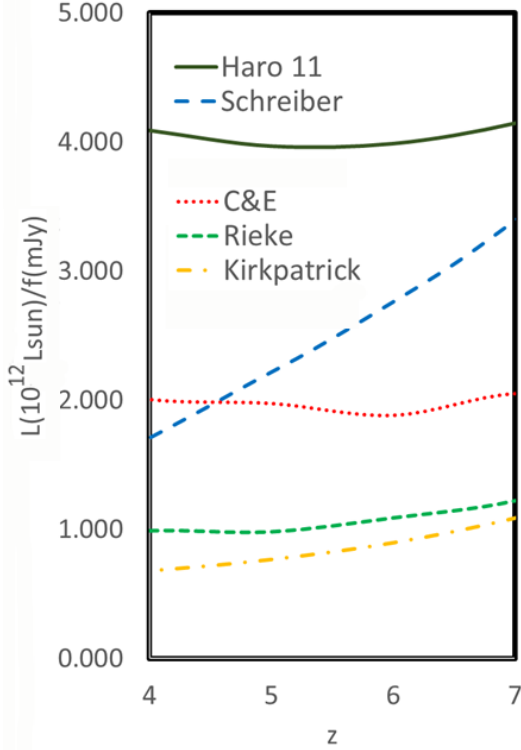


Figure 2: Conversion factors from ALMA observed Band 7 flux densities in mJy to $L(\text{TIR})$ in units of $10^{12} L_{\odot}$, for various SED templates: Schreiber et al. (2018); Rieke et al. (2009); Chary & Elbaz (2001); Kirkpatrick et al. (2015) and also with the Haro 11 template. The Rieke et al. (2009) template is applied as in Rujopakarn et al. (2013).

4. Conclusions

In this work, we compared observed FIR galaxy SEDs at $z \sim 6$ and theoretical predictions for the first massive Pop II galaxies. Our analysis is based on the dust model developed by De Rossi & Bromm (2017) but adapted to conditions reflecting the properties of luminous FIR galaxies at $z = 5 - 7$ (De Rossi et al., 2018).

The observed SEDs at $z \sim 6$ are broad and shifted to bluer wavelengths in comparison with SEDs associated with galaxies at lower z . The theoretical dust model is able to reproduce the observed trends as a consequence of the high energy densities of model massive Pop II galaxies and their dominant silicate dust composition. As discussed in De Rossi et al. (2018), the SED corresponding to the local galaxy Haro 11 constitutes a convenient proxy template to study galaxies at $z \gtrsim 5$.

The characterization of FIR galaxy SEDs at high z is

crucial for the exploration of the properties of the interstellar medium of high z galaxies. A straightforward application is the estimate of total FIR luminosities, which, once combined with the initial mass function, provide an estimate of the star formation rates in luminous dust-shrouded galaxies. Single-band ALMA measurements at ~ 1 mm are being used to infer IR luminosities and star formation rates at $z \approx 6$. However, the interpretation of such data depends on the adopted SED template as shown in Figure 2 (see also De Rossi et al., 2018). The non-blackbody nature for galaxy SEDs at $z \gtrsim 5$, predicted by our theoretical model and supported by the available measurements, needs to be considered to avoid an underestimation of total infrared luminosities and, hence, the star formation rates at these high redshifts.

Acknowledgements: MEDR thanks the Asociación Argentina de Astronomía for providing with partial financial support for attending its 61st annual meeting. The work of GHR, IS, and JL was partially supported by NASA Grant NNX13AD82G, and that of IS was also partially supported by a Hubble Fellowship. MEDR is grateful to PICT-2015-3125 of ANPCyT (Argentina) and also to María Sanz and Guadalupe Lucia for their help and support. VB acknowledges support from NSF grant AST-1413501. We thank Alexander Ji for providing tabulated dust opacities for the different dust models used here. This work makes use of the Yggdrasil code (Zackrisson et al., 2011), which adopts Starburst99 SSP models, based on Padova-AGB tracks (Leitherer et al., 1999; Vázquez & Leitherer, 2005) for Population II stars.

References

- Chary R., Elbaz D., 2001, ApJ, 556, 562
- Cherchneff I., Dwek E., 2010, ApJ, 713, 1
- De Rossi M.E., Bromm V., 2017, MNRAS, 465, 3668
- De Rossi M.E., et al., 2018, ApJ, 869, 4
- Faisst A.L., et al., 2017, ApJ, 847, 21
- Ji A.P., Frebel A., Bromm V., 2014, ApJ, 782, 95
- Kirkpatrick A., et al., 2015, ApJ, 814, 9
- Leitherer C., et al., 1999, ApJS, 123, 3
- Lyu J., Rieke G.H., Alberts S., 2016, ApJ, 816, 85
- Rieke G.H., et al., 2009, ApJ, 692, 556
- Rujopakarn W., et al., 2013, ApJ, 767, 73
- Schreiber C., et al., 2018, A&A, 609, A30
- Spilker J.S., et al., 2016, ApJ, 826, 112
- Vázquez G.A., Leitherer C., 2005, ApJ, 621, 695
- Zackrisson E., et al., 2011, ApJ, 740, 13